

Research Article

Open Access



Wind risk assessment of urban street trees based on wind-induced fragility

Yi Luo, Xiaoqiu Ai

Shanghai Institute of Disaster Prevention and Relief, Tongji University, Shanghai 200092, China.

Correspondence to: Dr. Xiaoqiu Ai, Shanghai Institute of Disaster Prevention and Relief, Tongji University, 1239 Siping Road, Shanghai 200092, China. E-mail: aixiaoqiu@tongji.edu.cn

How to cite this article: Luo Y, Ai X. Wind risk assessment of urban street trees based on wind-induced fragility. *Dis Prev Res* 2022;1:7. <https://dx.doi.org/10.20517/dpr.2022.05>

Received: 13 May 2022 **Revised:** 12 Oct 2022 **Accepted:** 17 Nov 2022 **Published:** 30 Nov 2022

Academic Editor: Naiyu Wang **Copy Editor:** Fangling Lan **Production Editor:** Fangling Lan

Abstract

The failure of urban street trees caused by strong winds and has several adverse effects on urban functions and public safety. This study developed a wind fragility model based on the mechanical analysis of urban street trees. The uncertainty of the important parameters involved in this model was quantified for species of interest. Specifically, the vine copula function was used to estimate the joint probability distribution of the geometric parameters. Furthermore, the tree fragility curves were obtained and then validated by the historical measured date. The proposed model may help in effectively identifying high-risk streets and regions.

Keywords: Urban street trees, wind risk assessment, fragility curves

INTRODUCTION

The breakage and falling of street trees caused by extreme winds may lead to direct economic losses and indirect impacts, such as the failure of structures, lifeline facilities, and traffic systems, which severely threaten the lives and properties of residents.

Existing studies on wind damage to trees can be roughly categorized into mechanistic and statistical approaches. The statistical approach directly estimates the probability of damage and the factors influencing tree failures from historical data using various regression and statistical techniques^[1,2]. However, because the



© The Author(s) 2022. **Open Access** This article is licensed under a Creative Commons Attribution 4.0 International License (<https://creativecommons.org/licenses/by/4.0/>), which permits unrestricted use, sharing, adaptation, distribution and reproduction in any medium or format, for any purpose, even commercially, as long as you give appropriate credit to the original author(s) and the source, provide a link to the Creative Commons license, and indicate if changes were made.



date used for statistical analysis is typically locally specific, it has not been confirmed whether the developed statistical model can be generalized^[3,4]. Moreover, statistical models face difficulties in elucidating the actual mechanism of wind effects on trees.

In contrast, the mechanistic approach is predominant in studies on wind-induced tree failure. As early as 1881, Greenhill investigated the stability of trees using a bottom-fixed tapered rod^[5]. Subsequently, researches on the mechanistic tree model developed toward two directions. One direction tends to develop increasingly more refined and sophisticated tree models^[6,7]. The finite element model considering precise tree geometry and wind-tree interaction is particularly popular^[8-14]. The other direction is more practical and application-oriented. It tends to use models with relatively simple geometry, and focuses on the specification and quantification of the key model parameters. Specifically, HWIND^[15], GALES^[16], and FOREOLE^[17] are the most widely investigated models. The three above-mentioned modeling approaches simplify the tree as a tapered rod and adopt quasi-static analysis^[18]. The widely acknowledged Hazus model for multi-hazard loss estimation^[19] involves a module for tree blowdown, whereby an individual tree is modeled as a single-degree-of-freedom (SDOF) oscillator. However, the accuracy of this model is still unsatisfactory.

To evaluate the wind risk, most mechanistic models, such as HWIND, GALES, and FOREOLE, resort to calculating the critical wind speed (CWS) required to cause the damage to an "average tree"^[18,20]. In contrast, the Hazus tree blowdown model estimates tree damage using the fragility curve, that is, by calculating the conditional failure probability corresponding to different wind speeds. Owing to the inherent randomness of tree morphology, the environment, and tree failure occurrence, this study adopted the fragility scheme for risk assessment.

However, almost all the above-mentioned studies have focused either on forest trees or simply on individual trees. Despite the severe and potentially catastrophic impact of urban tree failure^[21,22], and the significant differences between the wind environment and tree features of urban areas and forests^[23], few studies have established quantitative wind risk assessment models for urban trees^[24]. Studies focusing on trees in urban areas have practical significance, while the computational efficiency of the single-tree model is important for facilitating subsequent city-scale analysis.

This study developed a wind risk assessment model for trees in urban streets. To predict wind-induced failure, a mechanistic model based on the HWIND and GALES models is proposed. Further, focusing on the quantification of the involved uncertainties, the probability distributions of significant parameters were investigated in detail. Specifically, the joint probability distributions of the geometric parameters were estimated using the vine copula function, based on the data from an urban tree database. Finally, the tree fragility curves were obtained and validated.

MECHANISTIC WIND DAMAGE TREE MODEL

A mechanistic tree model for the deterministic analysis of a single tree subjected to wind loading is proposed. The proposed model combines the HWIND and GALES models, and involves the simplification of trees into a cantilever corresponding to the trunk, as shown in [Figure 1](#). The cantilever beam is separated into several elements. Each element is considered as a cylinder, and the wind load is considered to be uniformly distributed on each element. Subsequently, the internal force and stress of each node can be calculated and the tree damage can be assessed.

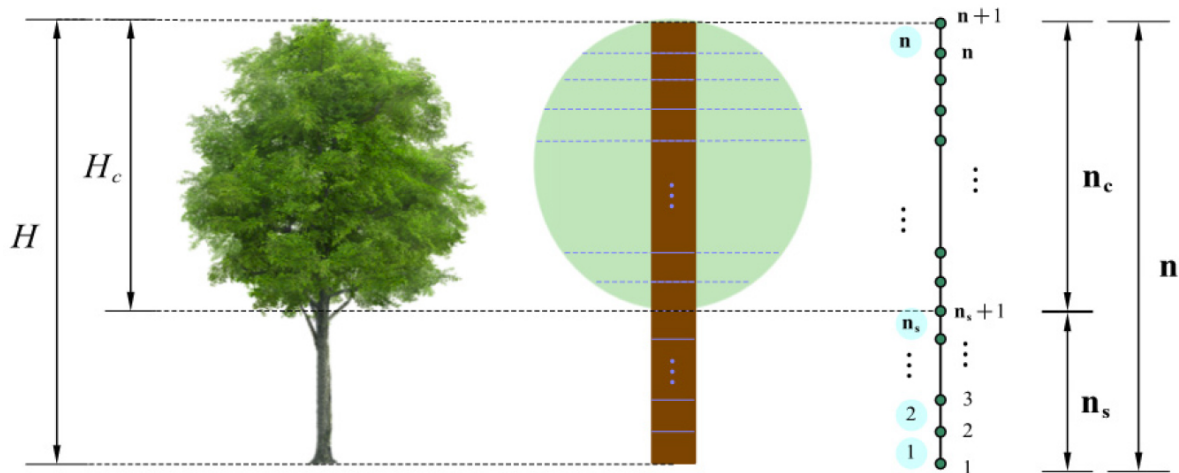


Figure 1. Diagram of tree model. H : tree height; H_c : crown height; n : number of elements; n_c : number of elements in crown area; n_s : number of elements in stem area.

Parameters of tree model

The basic parameters required to determine the proposed structural model are geometric and material parameters.

The three most fundamental geometric parameters of trees are the diameter at breast height (DBH), crown diameter (D_c), and crown height (H_c). All of them can be considered as random variables depending on the tree height and will be discussed in later sections.

Except for the three fundamental parameters, the taper equation of the trunk is essential for determining the element diameters. The proposed model adopts the widely used Max and Burkhart equation, which is expressed as follows^[25]:

$$\left(\frac{d_z}{DBH}\right)^2 = b_1 \times \left(\frac{z}{H} - 1\right) + b_2 \times \left[\left(\frac{z}{H}\right)^2 - 1\right] + b_3 \times \left(a_1 - \frac{z}{H}\right)^2 \times I_1 + b_4 \times \left(a_2 - \frac{z}{H}\right)^2 \times I_2 \quad (1)$$

where d_z denotes the stem diameter at height z ; b_1 , b_2 , b_3 , and b_4 are the shape parameters; a_1 is the relative height of the first knot, that is, the point of transition between a paraboloid and a cone in the upper part of the stem; a_2 is the relative height of the second point of transition between a neiloid and a paraboloid in the lower part; $I_1 = 1$ if $z/H < a_1$, otherwise $I_1 = 0$; $I_2 = 1$ if $z/H < a_2$, otherwise $I_2 = 0$.

The crown shape is an important geometric factor for tree modeling because it directly affects the estimated wind loads on trees. The following relationship is used to fit the crown profile^[26]:

$$\left(\frac{d_{ci}}{D_c}\right)^t + \left(\frac{i-0.5}{n_c}\right)^t = 1 \quad i = 1, 2, \dots, n_c \quad (2)$$

where d_{ci} denotes the crown diameter of the i -th element from the bottom of the crown; n_c is the number of elements in the crown area; t is the shape parameter. According to the US urban tree database^[27], most

conifers have a paraboloid crown, that is, they are widest at the bottom third of the crown. Herein, the shape parameter for conifers was considered as 1.4^[26], which satisfies the shape of a paraboloid. The dominant crown shape of broadleaf trees is ellipsoid; therefore, the shape parameter was considered to be equal to 2.

The material parameters include the stem density ρ_s , crown-to-stem weight ratio r_{cs} , and modulus of rupture σ_r . Species-varying random variables are considered. The values and distributions of these parameters are discussed below.

Loads on trees

The self-weight of trees is calculated using elements. For elements in the crown area, the weight of the element is the combination of the stem and crown weight. The weight of the stem can be determined from the stem density ρ_s and stem diameter at the height of each element. The weight of the crown can be calculated from the crown-to-stem weight ratio r_{cs} . Then, the crown weight is assigned to each crown-area element according to the crown diameter D_{ci} of that element.

The mean wind speed at the top of the tree \bar{U}_H can be obtained from the power law^[28] as follows:

$$\bar{U}_H = U_{10} \left(\frac{H}{10} \right)^a \quad (3)$$

where U_{10} is the 10-min mean wind speed at the height of 10 m, and a is the ground roughness coefficient. Hereafter, unless otherwise specified, all mean wind speeds are averaged over a 10-min period. Within the tree height, the mean wind speed can be calculated as follows^[10]:

$$\bar{U}(z) = \bar{U}_H \left(\frac{z}{H} \right)^{1/7} \quad (4)$$

Because quasi-static analysis is adopted for the proposed tree model, the effect of the fluctuating wind is considered by introducing a gust factor, as follows:

$$G_f = \frac{U_p}{\bar{U}}, \quad (5)$$

where U_p is the peak wind speed, and \bar{U} denotes the mean wind speed. The gust factor is considered as a random parameter and will be discussed in a later section.

The wind load on each element is represented by a point load concentrated at the center of the element, as follows:

$$F_i = \frac{1}{2} C_D \rho_a S_i A_i [U_p(z_i)]^2 \quad (6)$$

where C_D is the drag coefficient (for elements in the crown area, C_D is taken as 0.25 for broadleaf species, and 0.3 for conifers^[16,29]; otherwise, C_D is taken as 1^[29]); ρ_a denotes the air density and takes the value of 1.293 kg/m³ in this model; S_i is the dimensionless streamlining coefficient, and is given as follows^[16]:

$$S_i = \begin{cases} 0.8, & u(z) < 11\text{m/s} \\ (10/\bar{U}(z)) - 0.1, & 11\text{m/s} \leq \bar{U}(z) \leq 20\text{m/s} \\ 0.4, & u(z) > 20\text{m/s} \end{cases} \quad (7)$$

where $\bar{U}(z)$ is the mean wind speed at height z ; A_i is the area against the wind of the element; $U_p(z_i) = G_f \bar{U}$ denotes the peak wind speed at height z_i , and z_i is the height of the center of the element.

Failure determination

The overall and local failure of trees are considered. The overall failure includes the stem breakage mode and uprooting (or overturning) mode, while local failure refers to the branch breakage mode, which is typically more likely to occur compared with overall failure, but has a negative impact on the urban road environment as well.

Table 1 summarizes the specific failure criterion of each failure mode employed in this model. Notably, owing to the taper equation adopted herein, the element diameters shrink rapidly when approaching the canopy, as shown in **Figure 2A**. Consequently, for broadleaf species, the section stress along the tree height always exhibits a double-peak mode, as shown in **Figure 2B**, and the largest peak typically occurs at the second node from the top. It is clear that the overall breakage of the stem cannot be determined by this peak at the top area. Therefore, the model is divided into two parts: one corresponding to the trunk and the other corresponding to the branches. The midline of the crown is considered as the approximate boundary of these two regions.

The failure criterion for uprooting is expressed as follows:

$$M_{b, \text{crit}} < M_b \quad (8)$$

In this equation, the critical base moment $M_{b, \text{crit}}$ against uprooting can be determined as follows^[16]:

$$M_{b, \text{crit}} = C_{\text{reg}} W_s \quad (9)$$

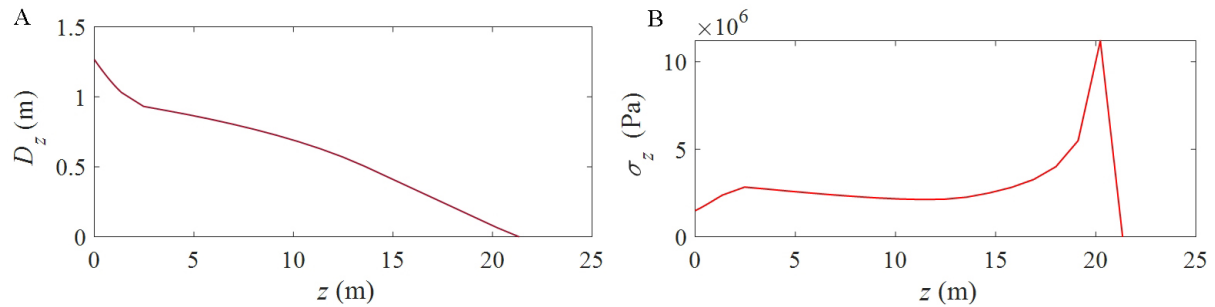
where W_s (kg) denotes the stem weight, and C_{reg} (Nm·kg⁻¹) is a regression constant that comprehensively reflects the root and soil characteristics. In the proposed model, C_{reg} is considered as a random variable, and its value and distribution are discussed later.

The bending moment of each node is obtained as follows:

$$M_i = \sum_{j=i+1}^{n+1} F_j (z_j - z_i) \quad (10)$$

Table 1. Description of failure modes

Failure category	Failure mode	Failure criterion
Overall Failure	Uprooting	Base bending moment (M_b) exceeds the critical uprooting moment ($M_{b, crit}$)
	Stem breakage	Maximum section stress in the trunk region ($\sigma_{max, s}$) exceeds the modulus of rupture (σ_r)
Local Failure	Branch breakage	Maximum section stress in the branch region ($\sigma_{max, b}$) exceeds the modulus of rupture (σ_r)

**Figure 2.** Typical section diameter and stress of broadleaf species. (A) Section diameter; (B) Section stress.

where F_j denotes the wind load given by Equation (6); n is the total number of elements, and the nodes are counted from the base to the top. Further, the base bending moment, which is also the maximum moment, is obtained as follows:

$$M_b = M_1 = \sum_{j=2}^n F_j z_j \quad (11)$$

Notably, the additional moment in the HWIND model, which accounts for the p-delta effect caused by the self-weight and wind-induced horizontal displacement, is not considered herein because the proposed model only considers the linear-elastic response of trees. Consequently, the additional moment is relatively small compared with the moment generated directly by the wind loads. Figure 3 shows the comparison between the additional moment and the direct moment from wind for $U_{10} = 40$ m/s. Note that, the additional moment increases with the wind speed. However, as can be seen, the additional moment is still negligible even for U_{10} up to 40 m/s. The simplification of neglecting the additional moment in the proposed model greatly reduces the computational costs. It is because it eliminates the calculation of structural displacement for the determination of the additional moment.

The failure criterion for stem breakage is expressed as follows:

$$\sigma_r < \sigma_{max, s} \quad (12)$$

where $\sigma_{max, s}$ is the maximum stress in the stem region, and is expressed as follows:

$$\sigma_{max, s} = \max(\sigma_i), \quad i = 1, 2, \dots, n - \langle n_c / 2 \rangle \quad (13)$$

where $\langle \cdot \rangle$ means rounding off to the nearest whole number; n_c is the number of elements in the crown region; σ_i denotes the stress at node i , and is expressed as follows^[29]:

$$\sigma_i = \frac{M_i d_i}{2I_i} + \frac{N_i}{A_i} \quad (14)$$

where d_i , A_i , and I_i denote the diameter, area, and moment of inertia of the stem cross section at node i , respectively; M_i can be calculated using Equation (10); N_i is the axial force caused by the self-weight.

The failure criterion for branch fracture is expressed as follows:

$$\sigma_r < \sigma_{\max, b} \quad (15)$$

where $\sigma_{\max, b}$ denotes the maximum stress in the stem region and is expressed as follows:

$$\sigma_{\max, s} = \max(\sigma_i), \quad i = n+1 - \langle n_c/2 \rangle, \dots, n+1 \quad (16)$$

QUANTIFICATION OF STOCHASTIC PARAMETERS

In this section, the stochastic parameters involved in the proposed mechanistic model are quantified. Specifically, the joint distributions of the geometric parameters are fitted using data from the USDA urban tree database^[27] via copula functions. However, owing to the lack of data, the probability distributions of material parameters are given empirically with mean values obtained from the literature. The distribution of the wind gust factor is identified from the time histories of the fluctuating winds generated using the Davenport spectrum^[30].

Because the geometric and material parameters of trees are species-dependent, to facilitate the model validation discussed in the next section, typical broadleaf trees and conifers were considered as the target species in this study. Notably, the same methodology can be applied to the analysis of other specific species when the corresponding information is provided.

Geometric parameters

The basic geometric parameters, that is, the diameters at breast height (DBH), crown diameter (D_c), and crown height (H_c) are estimated by the polynomial functions of the tree height (H).

The data used for regression were obtained from the USDA urban tree database^[26]. For each species, the regression parameters and the distribution of random variables were fitted. The model employed to fit the data points is expressed as follows:

$$y_i = f(x_i) \cdot \theta_i \quad (17)$$

where y_i is the i -th sample value of the parameter, and may refer to DBH , D_c , or H_c ; x_i is the tree height (H) of the i -th sample; $f(x)$ denotes the regression polynomial function; θ_i is the i -th sample value of the random variable corresponding to the considered parameter.

The distributions of random variables θ_{DBH} , θ_{D_c} , and θ_{H_c} are considered to be independent of the tree height H . Figure 4 shows the samples of θ_{DBH} , θ_{D_c} , and θ_{H_c} against H for various typical cases. For varying values of

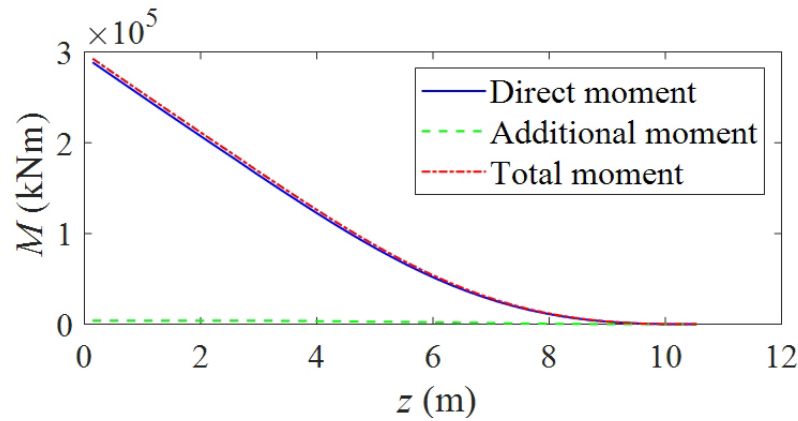


Figure 3. Comparison of additional moment and direct moment.

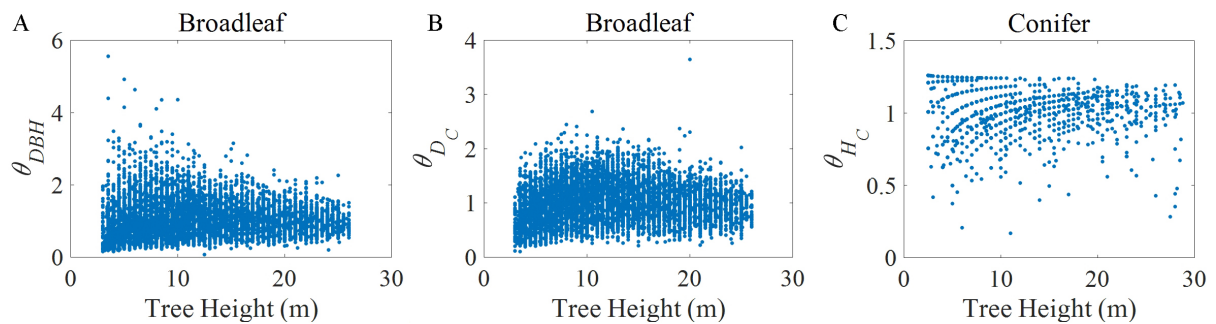


Figure 4. Part of data of geometric random variables θ_{DBH} , θ_{Dc} , and θ_{Hc} . DBH: diameter at breast height; D_c : crown diameter; H_c : crown height; θ : random variable corresponding to considered parameter. (A) θ_{DBH} of broadleaf species; (B) θ_{Dc} of broadleaf species; (C) θ_{Hc} of conifers.

H , all three random variables are approximately homoscedastic.

The linear polynomial function is employed for the regression of diameter at breast height (DBH) and crown height (H_c); the quadratic regression function is used for the crown diameter (D_c). The comparisons of the regression functions are presented in Figure 5, and the parameters obtained by the least squares algorithm are presented in Table 2. As shown in Figure 5, compared with the other two geometric random variables, the differences among the crown height (H_c) regression results for different species are relatively small, and the corresponding variance in the samples is the smallest.

Before constructing the joint distribution of the random variable using copula theory, the marginal distributions of the variables were determined. In this study, five distribution types, namely, the normal distribution, lognormal distribution, Gamma distribution, Weibull distribution, and Burr type XII distribution, were considered and fitted by the maximum likelihood estimation.

Figure 6 shows the fitting results for the distributions of typical broadleaf trees.

The D value in the Kolmogorov-Smirnov (K-S) test was used to determine the best-fitted distribution, as follows^[31]:

$$D = \max_x (|F(x) - S_n(x)|), \quad (18)$$

where $F(x)$ denotes the assumed cumulative density function (CDF) of random variable X , and $S_n(x)$ is the stepwise cumulative frequency function of the sample data. Table 3 gives the best-fitted distribution of each species and geometric random variable, and the corresponding parameters.

The joint distributions of the geometric random variables (θ_{DBH} , θ_{Dc} , and θ_{Hc}) for each species are estimated by copula theory. To determine the dominating variable for constructing the vine copula structure, the Pearson, Spearman, and Kendall correlation coefficients for each random variable pair of all considered species were calculated as presented in Table 4. As can be seen, the correlation between θ_{DBH} and θ_{Dc} is much stronger compared with the correlation between θ_{Hc} and any of these two random variables. Based on the discriminant formulae^[32] for independence determination, the independence hypotheses for random variable pairs [θ_{DBH} , θ_{Hc}] and [θ_{Dc} , θ_{Hc}] were rejected. Therefore, θ_{Hc} was still considered as dependent, and the vine copulas were used to construct the three-dimensional joint probability density function.

Herein, five copula function types were considered: the Ali-Mikhail-Haq (AMH) copula, Frank copula, Clayton copula, Gaussian copula, and t copula. According to the Akaike information criterion (AIC), the best-fitted copula has the minimum AIC value^[33]. For each random variable pair, the best-fitted copula functions and their parameters are presented in Table 5. Figure 7 shows the comparison between the original 11,567 data points and the 1000 samples generated by the estimated vine copula function and marginal distributions for broadleaf trees. As can be seen, the results are in good agreement.

Material Parameters and critical bending moment

In the proposed model, the random material and strength parameters of trees include the stem density ρ_s , modulus of rupture σ_r , crown-to-stem weight ratio r_{cs} , and regression coefficient of critical bending moment C_{reg} . Similar to the geometric parameters, these parameters are expressed as follows:

$$X = \bar{X} \cdot \theta \quad (19)$$

where X is a random material parameter and may refer to ρ_s , σ_r or r_{cs} ; \bar{X} denotes the mean value of the random parameter; θ is a random variable with a mean equal to 1, and the standard deviation is equal to the coefficient of variation of X .

The construction of accurate probabilistic distributions of the model parameters is always desirable. However, because a large data set of material parameters is not yet available, their distributions must be assumed based on experience. In the proposed model, the lognormal distribution is adopted for all random material and strength variables. The distribution parameters are determined by moment estimation; therefore, the mean value \bar{X} and the coefficient of variation of the parameters still need to be determined.

The USDA Wood Handbook^[34] provides the specific gravity (S_g) and modulus of rupture (σ_r) of various species. Notably, all material parameters in this model should take the value of green trees instead of overdried wood. With S_g of green trees, the stem density (ρ_s) can be obtained as follows:

$$\rho_s = (1 + MC) \times S_g \rho_w \quad (20)$$

Table 2. Regression parameters for different species and geometric parameters (for linear function, $f(x) = ax + b$; for quadratic function, $f(x) = ax^2 + bx + c$)

Species	DBH (cm)	D_c (m)	H_c (m)
Broadleaf	$a = 3.5857$ $b = -0.9613$	$a = -0.0144$ $b = 1.0950$ $c = -0.5046$	$a = 0.8424$ $b = -1.0316$
Conifer	$a = 2.8993$ $b = 4.9477$	$a = -0.0105$ $b = 0.7091$ $c = 0.8331$	$a = 0.8203$ $b = -0.1333$

DBH: Diameter at breast height; D_c : crown diameter; H_c : crown height.

Table 3. Best-fitted distribution and parameters of geometric random variables

Species	θ_{DBH}		θ_{D_c}		θ_{H_c}	
	Distribution	Parameters	Distribution	Parameters	Distribution	Parameters
Broadleaf	Burr	$\alpha = 1.0269$ $c = 3.7257$ $k = 1.3808$	Burr	$\alpha = 1.3840$ $c = 4.0562$ $k = 3.2724$	Burr	$\alpha = 1.1243$ $c = 9.0512$ $k = 2.1530$
Conifer	Burr	$\alpha = 1.3891$ $c = 3.1537$ $k = 2.7291$	Gamma	$a = 6.4717$ $b = 0.1527$	Weibull	$a = 1.0626$ $b = 7.9837$

DBH: Diameter at breast height; D_c : crown diameter; H_c : crown height; θ_i : random variable corresponding to considered parameter.

Table 4. Correlation coefficients for each random variable pair

Type of corr. coeff.	Random variable pairs	Broad-leaf	Conifer
Pearson	$[\theta_{DBH}, \theta_{D_c}]$	0.659	0.705
	$[\theta_{DBH}, \theta_{H_c}]$	-0.173	-0.088
	$[\theta_{D_c}, \theta_{H_c}]$	-0.144	-0.100
Spearman	$[\theta_{DBH}, \theta_{D_c}]$	0.711	0.729
	$[\theta_{DBH}, \theta_{H_c}]$	-0.182	-0.087
	$[\theta_{D_c}, \theta_{H_c}]$	-0.135	-0.152
Kendall	$[\theta_{DBH}, \theta_{D_c}]$	0.525	0.545
	$[\theta_{DBH}, \theta_{H_c}]$	-0.124	-0.060
	$[\theta_{D_c}, \theta_{H_c}]$	-0.091	-0.103

DBH: Diameter at breast height; D_c : crown diameter; H_c : crown height; θ_i : random variable corresponding to considered parameter.

Table 5. Best fitted copula function and their parameters

Species	(u_{DBH}, u_{D_c})		(u_{DBH}, u_{H_c})		$(w_{D_c DBH}, w_{H_c DBH})$	
	Copula	Parameters	Copula	Parameters	Copula	Parameters
Broadleaf	t	$\rho = 0.7256$ $\nu = 8.7194$	t	$\rho = -0.1937$ $\nu = 7.8419$	t	$\rho = -0.6687$ $\nu = 31.3205$
Conifer	Frank	$\theta = 6.6617$	t	$\rho = -0.0962$ $\nu = 7.2625$	Frank	$\theta = -0.0624$

DBH: Diameter at breast height; D_c : crown diameter; H_c : crown height.

where MC denotes the moisture content of the green trees of the specific species considered, and $\rho_w = 1000 \text{ kg/m}^3$ is the density of water.

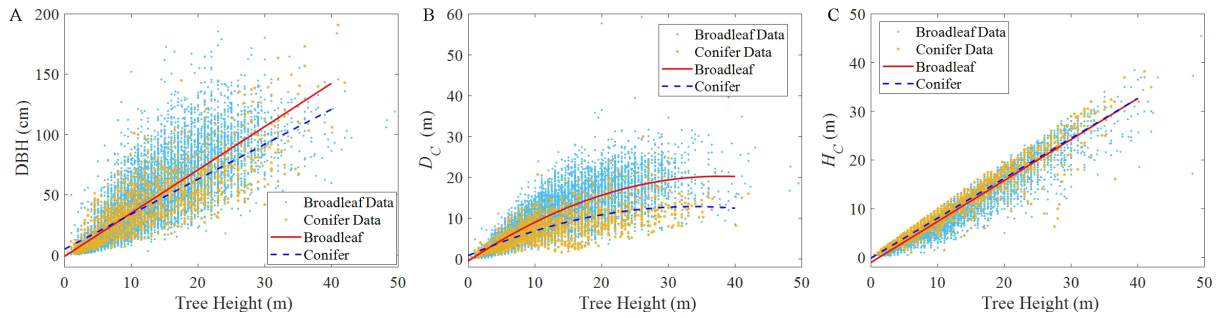


Figure 5. Regression results for DBH , D_c , and H_c of different species. DBH : diameter at breast height; D_c : crown diameter; H_c : crown height. (A) diameter at breast height DBH ; (B) crown diameter D_c ; (C) crown height H_c .

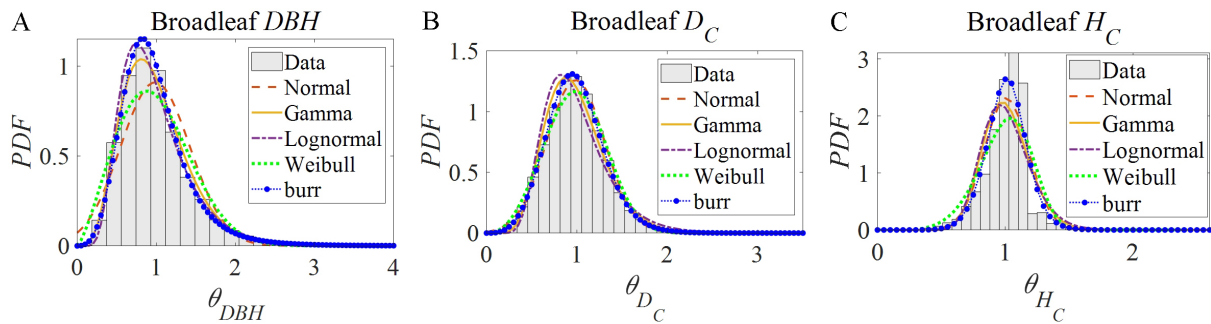


Figure 6. Fitting results for assumed marginal distributions of geometric random variables of broadleaf trees. DBH : diameter at breast height; D_c : crown diameter; H_c : crown height; θ : random variable corresponding to considered parameter. (A) diameter at breast height θ_{DBH} ; (B) crown diameter θ_{D_c} ; (C) crown height θ_{H_c} .

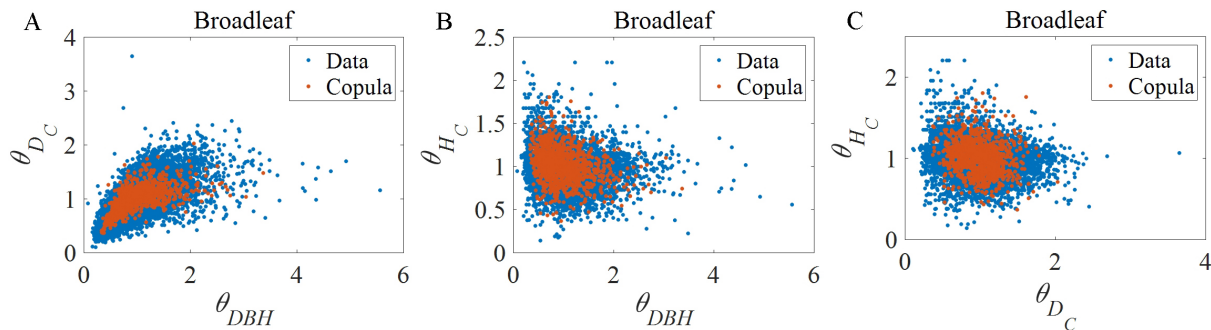


Figure 7. Comparison of samples generated by copula function and original data. DBH : diameter at breast height; D_c : crown diameter; H_c : crown height; θ : random variable corresponding to considered parameter. (A) $[\theta_{DBH}, \theta_{D_c}]$; (B) $[\theta_{DBH}, \theta_{H_c}]$; (C) $[\theta_{D_c}, \theta_{H_c}]$.

The mean values of MC , S_g , ρ_s , and σ_r are listed in Table 6. Herein, the mean and coefficients of variation for the above-mentioned material parameters of typical broadleaf trees (or conifers) are estimated by the data of all available hardwood (or softwood) species in the USDA Wood Handbook, and each species has the same weight in the computation.

Owing to the lack of supporting materials, the crown-to-stem weight ratio r_{cs} is not considered as species-dependent. The crown weight is approximately $28.0\% \pm 3.3\%$ of the fresh weight of an entire tree^[35]; therefore, r_{cs} is approximately $39\% \pm 6.5\%$. Consequently, in this study, the mean r_{cs} value was considered as 0.39, and the coefficient of variation was considered as 0.167.

Table 6. Mean values of MC, S_g , ρ_s , and σ_r of different species

Species	MC (%)	S_g	ρ_s (kg/m ³)	σ_r (10 ⁷ Pa)
Broadleaf	86	0.517	923.9	5.57
Conifer	105	0.401	802.2	4.34

MC: Moisture content of green trees of specific considered species; ρ_s : stem density; S_g : specific gravity; σ_r : modulus of rupture.

The regression coefficient C_{reg} of the critical base moment for uprooting failure is also species-dependent. Many experimental studies have been conducted to measure the value of C_{reg} for different species and various root and soil conditions^[16,20,29,36-38]. In previous studies, the value of C_{reg} varied from 67 to more than 200. However, owing to the enormous experimental cost of measuring C_{reg} , the data of C_{reg} are still limited to an extent that makes it rather difficult to obtain a reasonable distribution of C_{reg} for different species and the root and soil properties. Therefore, in this study, C_{reg} was only considered as species-dependent. The mean values of C_{reg} for general broadleaf species and conifers are identified in the following model validation procedure, respectively, and the standard deviation of $\theta_{C_{reg}}$ was set to 0.2.

The conclusions regarding the random variables for the stem density, modulus of rupture, crown-to-stem weight ratio, and regression coefficient of the critical base moment, that is, θ_{ρ_s} , θ_{σ_r} , $\theta_{r_{cs}}$ and $\theta_{C_{reg}}$, respectively, are presented in Table 7.

Gust factor

In this study, the gust factor was calculated by the ratio of the 1-second gust to the 10-min mean wind speed. The fluctuating wind speed can be considered as a Gaussian stationary process. For an initial variate satisfying the Gaussian distribution $N(\mu, \sigma)$, the maximum value obtained for samples with size n satisfies the Gumbel distribution for large n ^[31]. For the gust factor G_f in Equation (5), its corresponding initial variate satisfies $N(1, I_{10})$, where I_{10} denotes the coefficient of variation of the wind speed at the height of 10 m. Therefore, the distribution of G_f can be obtained as follows:

$$F_{G_f}(y) = \exp\left[-e^{-a_n(y-u_n)}\right] \quad (21)$$

where $F_{G_f}(y)$ denotes the CDF of G_f and the following relationships hold:

$$\begin{aligned} u_n &= I_{10} \left(\sqrt{2 \ln n} - \frac{\ln \ln n + \ln(4\pi)}{2\sqrt{2 \ln n}} \right) + 1 \\ a_n &= \frac{\sqrt{2 \ln n}}{I_{10}} \end{aligned} \quad (22)$$

As can be seen, if I_{10} is known, the distribution of G_f can be fully determined with sample size n . According to China's specification for the design load of buildings (GB 50009-2012), for urban areas with dense building clusters, I_{10} can be taken as 0.23^[39]. Then, the following empirical value of n is used in this model:

$$n = 100 \left(\log_2 \left(4 \frac{\bar{U}_{10}}{5} \right) \right) \quad (23)$$

Table 7. Random variables of material and strength properties

Random variable	Distribution	Mean/Standard deviation
$\theta\rho_s$	Lognormal	$\mu = 1, \sigma = 0.1403$ (Broadleaf) $\mu = 1, \sigma = 0.1403$ (Conifer)
$\theta\sigma_r$	Lognormal	$\mu = 1, \sigma = 0.2499$ (Broadleaf) $\mu = 1, \sigma = 0.2499$ (Conifer)
θr_{cs}	Lognormal	$\mu = 1, \sigma = 0.167$
θC_{reg}	Lognormal	$\mu = 1, \sigma = 0.2$

ρ_s : Stem density; σ_r : modulus of rupture; r_{cs} : crown-to-stem weight ratio; C_{reg} : regression coefficient; θ : random variable corresponding to considered parameter.

For each \bar{U}_{10} , Eq. (23) is approximated from 10,000 time series with a 10-min period and the sampling frequency of 1 Hz, as determined by the corresponding Davenport Spectrum^[30]. Notably, there are other distributions of instantaneous maximum wind speed that similarly have a double exponential form. These distributions also require the estimation of certain parameters when applied to the quasi-static analysis^[40]. All of these distributions are reasonable approximations when the sample size n is large. Therefore, this study adopted the widely used Gumbel distribution.

WIND FRAGILITY AND MODEL VALIDATION

The probabilistic mechanical model was validated in the same manner using the same survey data as the Hazus model.

In the technical manual of Hazus-MH 2.1, the blowdown results for 1158 trees (628 conifer and 530 deciduous trees) in eight residential subdivisions in eastern North Carolina caused by Hurricane Isabel in 2003, and the estimated peak gust wind speed of each subdivision, are provided^[19]. Trees are divided into conifers and deciduous trees by species, and into four classes by height, amounting to a total of eight classes. Because the sample size at each surveyed site is not sufficient to allow a reasonable estimation of the failure property if considered separately, the Hazus manual proposes a weighted average scheme to make use of these measured data^[19]. For each tree class at all surveyed sites, the weighted average blowdown probability for trees, and the corresponding weighted wind speed, were calculated as indicated by the star symbol in Figure 8. The model will be validated if, for all tree classes, the estimated fragility curve passes through the corresponding weighted average point. Notably, only the estimated peak gust wind speed of each site is provided, while the proposed model is based on the mean wind speed. Therefore, the mean wind speed of each site can be further estimated using the following expression:

$$\bar{U}_{10} = U_p / (1 + gI_u) \quad (24)$$

where U_p denotes the provided peak wind speed; g denotes the peak factor, and is considered as 3.0 in accordance with the Hazus manual^[19]; I_u denotes the turbulence intensity and was considered to be the same as I_{10} for an urban area, that is, equal to 0.23.

By employing the proposed model, the failure probability P_f at each \bar{U}_{10} was calculated by Monte Carlo simulation with 10,000 samples. The proposed mechanistic model has fairly high efficiency, and the computation of one fragility curve takes no more than one second. Therefore, the proposed model can be easily extended to city-scale when various tree species, tree heights, and other dominant tree properties must be considered separately.

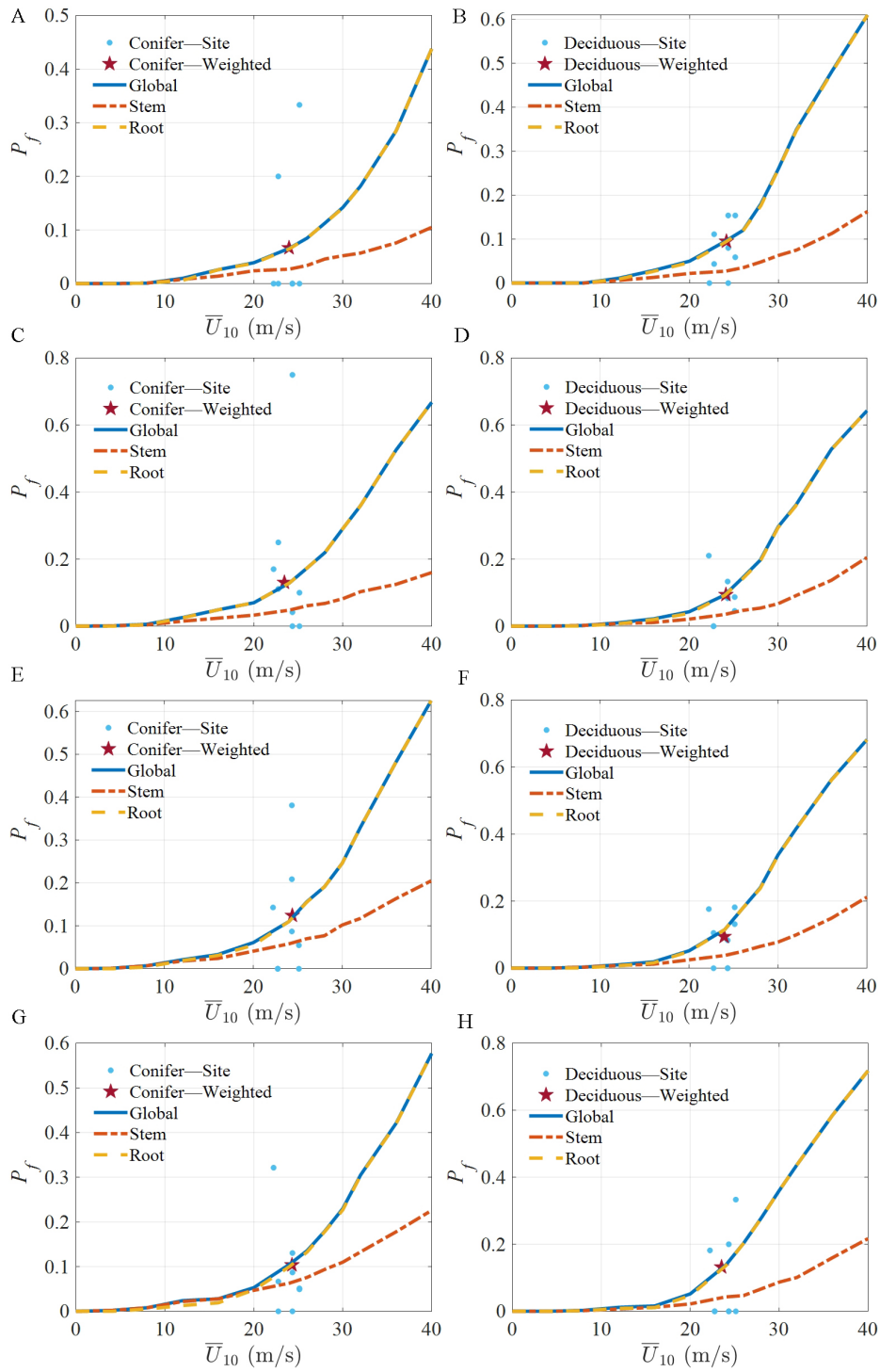


Figure 8. Model validation results. H : tree height; C_{reg} : regression coefficient; P_f : failure probability; U_{10} : mean wind speed in 10 min at height of 10 m. (A) Coniferous tree, $H = 20$ feet (6.1 m), $\bar{C}_{reg} = 130$; (B) Deciduous tree, $H = 20$ feet (6.1 m), $\bar{C}_{reg} = 160$; (C) Coniferous tree, $H = 35$ feet (10.7 m), $\bar{C}_{reg} = 120$; (D) Deciduous tree, $H = 35$ feet (10.7 m), $\bar{C}_{reg} = 180$; (E) Coniferous tree, $H = 50$ feet (15.2 m), $\bar{C}_{reg} = 145$; (F) Deciduous tree, $H = 50$ feet (15.2 m), $\bar{C}_{reg} = 180$; (G) Coniferous tree, $H = 70$ feet (21.3 m), $\bar{C}_{reg} = 165$; (H) Deciduous tree, $H = 70$ feet (21.3 m), $\bar{C}_{reg} = 180$.

The survey data and estimation results for eight tree classes are shown in Figure 8. Because only the height ranges of four tree height classes are available, and there is no information on the specific height of each sample tree, a representative height was selected for each height class. The tree height information of the validation data is initially given in feet. In Figure 8, the representative heights measured in feet and meters are given simultaneously. Because the survey did not provide data for the local damage of trees, this failure mode was not considered in the model validation. Recall that the mean values of C_{reg} (denoted by \bar{C}_{reg}) still need to be determined. The \bar{C}_{reg} value used in the estimation of each tree class is noted in the corresponding subplot in Figure 8. All estimated \bar{C}_{reg} values lie within a reasonable range, which indicates the rationality of the proposed model.

Another phenomenon observed in the estimation is that the dominant failure mode is uprooting at the weighted wind speed. Actually, there is certain regularity between the dominant failure mode estimated by the proposed model and the wind speed. When the wind speed is low, the dominant failure mode is stem fracture, while the failure probability in this stage is typically too low to be heeded. When the wind speed increases, the trees are more likely to fail at the root.

As a further exploration, the significance of the correlation of random model parameters, that is, the necessity of applying the vine copula functions, was investigated. As shown in Figure 9, there is a significant difference between the fragility curves obtained by the proposed vine copula function and those obtained from independent geometric parameters with the same marginal distributions. Undoubtedly, this demonstrates the necessity of considering the correlation of random parameters and the advantage of applying the vine copula function in the proposed model. Moreover, it shows that the probability distributions of model parameters are very important to fragility analysis; therefore, future studies should pay more attention to this issue.

CONCLUDING REMARKS

This paper proposes a wind risk assessment model for trees in urban streets. Specifically, based on a mechanistic tree model with elaborated considerations of the model parameter uncertainties, a probabilistic model for calculating the fragility of urban street trees was established. By using a sufficient amount of available data, the joint probability distributions of the fundamental geometric parameters of trees were obtained based on the vine copula theory. Moreover, the wind fragility curves of typical broadleaf trees and conifers were obtained. The comparison of the results obtained by the proposed model to survey data confirmed the validity of the proposed model.

The significance of accurate probability modeling in risk assessment was emphasized. In addition to the marginal probability distribution of each parameter, the correlation and dependence of parameters are also important. Copula functions provide a feasible approach toward accurately constructing the joint distributions of random parameters using parametric and explicit expressions.

The proposed mechanistic model is fairly efficient and is expected to be applied to wind risk assessment at the city scale. However, owing to the lack of data, there are still many deficiencies in the parameter quantification and model validation of the current model. Issues to be further improved include the following: (1) accurate modeling of the distribution of material and strength parameters with the support of more experimental data; (2) considering the influence of root characteristics and root-soil interaction; and (3) comprehensive validation of proposed model with the support of additional survey data and refined numerical analysis.

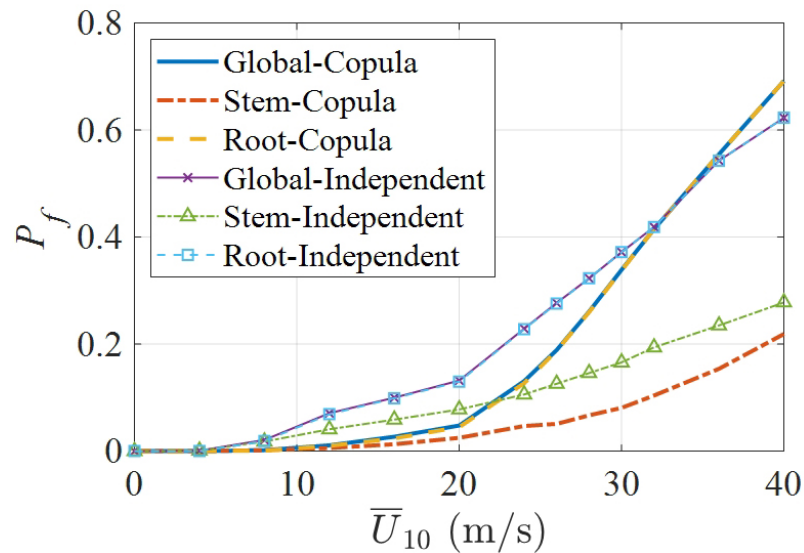


Figure 9. Comparison of fragility curves of typical deciduous tree. P_f : failure probability; U_{10} : mean wind speed in 10 min at height of 10 m.

DECLARATIONS

Authors' contributions

Performed data gathering and analysis work: Luo Y

Designed the research work and provided guidance: Ai X

Availability of data and materials

Not applicable.

Financial support and sponsorship

None.

Conflicts of interest

Both authors declared that there are no conflicts of interest.

Ethical approval and consent to participate

Not applicable.

Consent for publication

Not applicable.

Copyright

© The Author(s) 2022.

REFERENCES

1. Kabir E, Guikema S, Kane B. Statistical modeling of tree failures during storms. *Reliab Eng Syst Saf* 2018;177:68-79. [DOI](#)
2. Hart E, Sim K, Kamimura K, Meredieu C, Guyon D, Gardiner B. Use of machine learning techniques to model wind damage to forests. *Agric For Meteorol* 2019;265:16-29. [DOI](#)
3. Kamimura K, Gardiner B, Dupont S, Guyon D, Meredieu C. Mechanistic and statistical approaches to predicting wind damage to individual maritime pine (*Pinus pinaster*) trees in forests. *Can J For Res* 2015;46:88-100. [DOI](#)
4. Gardiner B. Wind damage to forests and trees: a review with an emphasis on planted and managed forests. *J For Res* 2021;26:248-66.

DOI

5. James KR, Haritos N, Ades PK. Mechanical stability of trees under dynamic loads. *Am J Bot* 2006;93:1522-30. DOI PubMed
6. Morgan J, Cannell MGR. Structural analysis of tree trunks and branches: tapered cantilever beams subject to large deflections under complex loading. *Tree Physiol* 1987;3:365-74. DOI PubMed
7. Baker CJ. The development of a theoretical model for the windthrow of plants. *J Theor Biol* 1995;175:355-72. DOI
8. Sellier D, Fourcaud T, Lac P. A finite element model for investigating effects of aerial architecture on tree oscillations. *Tree Physiol* 2006;26:799-806. DOI PubMed
9. Moore JR, Maguire DA. Simulating the dynamic behavior of Douglas-fir trees under applied loads by the finite element method. *Tree Physiol* 2008;28:75-83. DOI PubMed
10. Ciftci C, Arwade SR, Kane B, Brena SF. Analysis of the probability of failure for open-grown trees during wind storms. *Probabilist Eng Mech* 2014;37:41-50. DOI
11. Ciftci C, Brena SF, Kane B, Arwade SR. The effect of crown architecture on dynamic amplification factor of an open-grown sugar maple (*Acer saccharum* L.). *Trees Struct Funct* 2013;27:1175-89. DOI
12. Ai X, Cheng Y, Peng Y. Nonlinear dynamics and failure wind velocity analysis of urban trees. *Wind Struct An Int J* 2016;22:89-106. DOI
13. Peng Y, Wang Z, Ai X. Wind-induced fragility assessment of urban trees with structural uncertainties. *Wind Struct An Int J* 2018;26:45-56. DOI
14. Moravčík L, Vincúr R, Rózová Z. Analysis of the static behavior of a single tree on a finite element model. *Plants* 2021;10:1284. DOI PubMed PMC
15. Peltola H, Kellomäki S, Väisänen H, Ikonen VP. A mechanistic model for assessing the risk of wind and snow damage to single trees and stands of Scots pine, Norway spruce, and birch. *Can J For Res* 1999;29:647-61. DOI
16. Gardiner B, Peltola H, Kellomäki S. Comparison of two models for predicting the critical wind speeds required to damage coniferous trees. *Ecol Modell* 2000;129:1-23. DOI
17. Ancelin P, Courbaud B, Fourcaud T. Development of an individual tree-based mechanical model to predict wind damage within forest stands. *For Ecol Manag* 2004;203:101-21. DOI
18. Gardiner B, Byrne K, Hale S, et al. A review of mechanistic modelling of wind damage risk to forests. *Forestry* 2008;81:447-63. DOI
19. Federal Emergency Management Agency (FEMA). Multi-hazard Loss Estimation Methodology Hurricane Model Hazus®-MH 2.1 Technical Manual. 2012. Available from: https://www.fema.gov/sites/default/files/2020-09/fema_hazus_hurricane-model_technical-manual_2.1.pdf [Last accessed on 30 Nov 2022].
20. Achim A, Ruel JC, Gardiner BA, Laflamme G, Meunier S. Modelling the vulnerability of balsam fir forests to wind damage. *For Ecol Manag* 2005;204:37-52. DOI
21. Jim CY, Liu HHT. Storm damage on urban trees in Guangzhou, China. *Landsc Urban Plan* 1997;38:45-59. DOI
22. Haafteen MA, Meuwissen MPM, Gardebroek C, Kopinga J. Trends in financial damage related to urban tree failure in the Netherlands. *Urban For Urban Green* 2016;15:15-21. DOI
23. Gardiner B, Berry P, Moulia B. Review: wind impacts on plant growth, mechanics and damage. *Plant Sci* 2016;245:94-118. DOI PubMed
24. Gu D, Zhao P, Chen W, Huang Y, Lu X. Near real-time prediction of wind-induced tree damage at a city scale: simulation framework and case study for Tsinghua University campus. *Int J Disaster Risk Reduct* 2021;53. DOI
25. Max T, Burkhart H. Segmented polynomial regression applied to taper equations. *For Sci* 1976;22:283-9. Available from: <https://academic.oup.com/forestscience/article-abstract/22/3/283/4675818> [last accessed on 17 Nov 2022]
26. Rautiainen M, Möttöus M, Stenberg P, Ervasti S. Crown envelope shape measurements and models. *Silva Fenn* 2008;42:19-33. DOI
27. McPherson EG, van Doorn N, Peper PJ. Urban tree database and allometric equations. USDA Forest Service 2016. DOI
28. Simiu E, Yeo DH. Wind effects on structures: modern structural design for wind. 4th ed. Hoboken: John Wiley & Sons. 2019.
29. Hou G, Chen S. Probabilistic modeling of disrupted infrastructures due to fallen trees subjected to extreme winds in urban community. *Nat Hazards* 2020;102:1323-50. DOI
30. Davenport AG. The spectrum of horizontal gustiness near the ground in high winds. *Quart J Roy Meteorol Soc* 1961;87:194-211. DOI
31. Ang AH-S, Tang WH. Probability concepts in engineering: emphasis on applications to civil and environmental engineering. 2nd ed. Hoboken: John Wiley & Sons. 2007.
32. Genest C, Favre AC. Everything you always wanted to know about copula modeling but were afraid to ask. *J Hydrol Eng* 2007;12:347-68. DOI
33. Tao J, Chen J, Ren X. Copula-based quantification of probabilistic dependence configurations of material parameters in damage constitutive modeling of concrete. *J Struct Eng* 2020;146:04020194. DOI
34. Ross RJ. Wood handbook: wood as an engineering material. 2010. DOI
35. Sader SA. Forest biomass, canopy structure, and species composition relationships with multipolarization L-band synthetic aperture radar data. *Photogramm Eng Remote Sensing* 1987;53:193-202. Available from: http://www.asprs.org/wp-content/uploads/pers/1987journal/feb/1987_feb_193-202.pdf [last accessed on 17 Nov 2022]
36. Nicoll BC, Gardiner BA, Rayner B, Peace AJ. Anchorage of coniferous trees in relation to species, soil type, and rooting depth. *Can J For Res* 2006;36:1871-83. DOI
37. Nicoll BC, Gardiner BA, Peace AJ. Improvements in anchorage provided by the acclimation of forest trees to wind stress. *Forestry*

- 2008;81:389-98. [DOI](#)
38. Locatelli T, Tarantola S, Gardiner B, Patenaude G. Variance-based sensitivity analysis of a wind risk model - Model behaviour and lessons for forest modelling. *Environ Model Softw* 2017;87:84-109. [DOI](#)
 39. MHUDPRC (Ministry of Housing and Urban-Rural Development of the People's Republic of China). Load code for the design of building structures. GB 50009-2012. Beijing: MHUDPRC; 2012. (in Chinese). Available from: https://www.mohurd.gov.cn/gongkai/fdzdgknr/tzgg/201207/20120723_210754.html [last accessed on 17 Nov 2022].
 40. Davenport AG. Note on the distribution of the largest value of a random function with application to gust loading. *Proc Inst Civ Eng* 1964;28:187-96. [DOI](#)